Solid–Liquid Phase Diagrams of Binary Aromatic Hydrocarbon Mixtures from Calorimetric Studies

Wahyudi B. Sediawan,[†] **Sumnesh Gupta, and Edward McLaughlin***

Department of Chemical Engineering, Louisiana State University, Baton Rouge, Louisiana 70803-7303

Solid–liquid phase diagrams of binary mixtures of aromatic hydrocarbons have been obtained from calorimetric studies. The sample of the binary solid mixture is heated at a constant rate until the solid is completely melted. During that process, the heat flux needed is monitored. By examination of the curves of the heat flux versus temperature, the solid–liquid phase diagrams can be constructed. Three binary systems (fluorene–dibenzofuran, dibenzothiophene–dibenzofuran, fluorene–dibenzothiophene) have been studied. It turns out that the fluorene–dibenzofuran system forms a solid solution at any composition, while dibenzothiophene–dibenzofuran and fluorene–dibenzothiophene systems have immiscibility gaps in the solid phases.

Introduction

The study of solid–liquid equilibrium is an important tool in analyzing some chemical engineering processes, such as crystallization and extraction, that can be used for chemicals such as aromatic hydrocarbons, which have relatively high melting points. Aromatic hydrocarbons are important components of heavier feedstocks (*1*) and coal liquids (*2*, *3*) which are gaining importance in the petrochemical industry. In this study, we examined the solid–liquid equilibria of three binary systems of aromatic hydrocarbons (fluorene–dibenzofuran, dibenzothiophene–dibenzofuran, fluorene–dibenzothiophene), via calorimetric studies.

The basic thermodynamic theory of phase equilibria can be directly applied to solid–liquid equilibria. The theory says that, at equilibrium, the fugacity of each component in one phase should be the same as its value in the other phases. A possible way of connecting the component fugacity to observable quantities is to use the activity coefficient approach. In solid–liquid equilibria, the ratio of the fugacities of the pure solid and liquid at the reference-state conditions, which is needed in the activity coefficient approach, can be calculated from the physical properties (heat of fusion, solid and liquid heat capacity, melting point) of the pure component (*4*).

The simplest case of solid–liquid equilibria is when the solid does not form a solid solution (simple eutectic diagram). In this case, the mole fraction of the component in the solid phase is unity, and so is its activity coefficient. In order to predict the solid–liquid equilibria for this system, the quantity needed is the liquid-phase activity coefficients provided the physical properties of the pure components are available (*5–7*).

In the case where solid solution occurs at any composition, the solid–liquid phase diagram can be predicted if the equations of the activity coefficients in the solid and liquid phases are available (*4*) together with the physical properties of the pure components.

In the more complex situation, in which the solid may consist of more than one phase, predictions become very difficult. Not only do the activity coefficients in each phase need to be known, but which phases will occur at a certain composition should also be determined.

For a given system, we do not know what kind of situation will happen. As an approximation, we can assume that if the sizes and shapes of the molecules are quite different, they will form a simple eutectic system. But in most cases, this is a poor approximation (*4*).

In this study, we examined three binary systems of aromatic hydrocarbons, to contribute data on the solid–liquid equilibria of aromatic hydrocarbons. We believe that the availability of data not only benefits industrial purposes but also supports the development of solid–liquid equilibrium theories, especially for aromatic hydrocarbons.

Experimental Section

The chemicals used were purchased from Aldrich Chemicals. The dibenzofuran and dibenzothiophene were dissolved in toluene and then recovered by recrystallization in a rotary evaporator. The purities obtained were 99.55% for dibenzofuran and 99.45% for dibenzothiophene. Those purities were determined by gas chromatography. The fluorene was used directly, without purification, since the purity obtained by the same analysis was 99.6%. The structures of those molecules are shown in Figure 1.

The phase diagrams were obtained by using a C-80 Setaram calorimeter, which is based on heat conduction, or the Tian-Calvet principle, and operates on the power compensated method (*8*). Calorimetry has long been used in determination of phase diagrams (*8*, *9*). New calorimeter design and better instrumentation now available have improved the accuracy and made the operation easier and faster. The calorimeter used consists of two identical and independent heat-flow detectors, which are surrounded by a heat-conducting block. The temperature of the block is controlled precisely by a temperature programmer/controller. The heat-flow detectors transfer heat to the two identical tubes. The sample is placed in one of the tubes, while the other tube is kept empty. The heat-flow detectors are made of high thermal conductivity materials, so that the temperatures of the block and the tube were almost identical. The detectors are differentially connected, so that the thermal perturbations to the block are eliminated, and only the signal due to heat exchange with the sample is generated.

In order to construct the phase diagrams, a test of a solid mixture of known composition, which has been melted and quickly solidified, was heated at a constant rate (around 0.02 K/min). During the process, the heat flux to the sample was monitored. Because of the heat effect during the phase transition, we could determine the initial and final temperatures at which the phase transition occurred (solidus and liquidus). The phase diagram can be constructed by doing many experiments using samples with various compositions.

The temperatures recorded during the experiment were the temperatures set by the programmer/controller (programmed temperature). Although the temperature of the sample was very close to the programmed temperature, the difference between them was calibrated. A thermometer was put in the sample tube filled with a small amount of ethylene glycol, and

---

[†] Permanent address: Jurusan Teknik Kimia, Universitas Gadjah Mada, Yogyakarta, Indonesia.

0021-9568/89/1734-0223$01.50/0

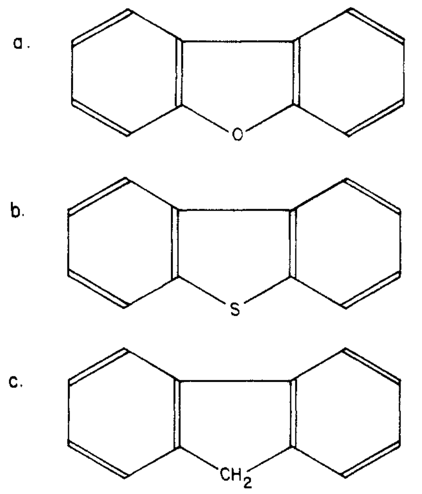

Figure 1. Molecular structures of dibenzofuran (a), dibenzothiophene (b), and fluorene (c).

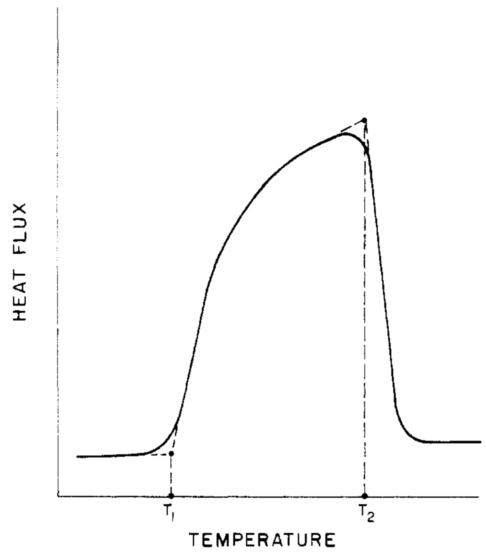

Figure 2. Schematic diagram of the heat flux versus temperature of a system that forms a solid solution.

the temperature of the calorimeter was increased at a constant rate (0.02 K/min), the rate used to determine the phase diagrams. During that process, the temperature differences between the programmed temperatures and the temperatures observed by the thermometer were monitored. It turns out that, within the range of the experimental temperatures, the temperatures of the sample were approximately 0.9 K below the programmed temperatures. The temperatures of the phase diagrams were then corrected by that number. We believe that the errors of the experiments (T_1, T_2) are within ±0.3 K.

The curves of heat flux versus temperature not only give the initial and final temperatures of the phase transition but also show the type of phase transition encountered. Figure 2 shows the heat flux versus temperature curve for the melting of a solid which is a solution. In this curve, T_1 is the temperature of the beginning of the phase transition and T_2 is the final temperature. The gradual change in signal clearly shows the solid phase to be an impure one and form a solid solution. As the temperature is raised, at T_1 the solid solution starts melting and this is in equilibrium with the liquid. Finally, at T_2 all the solid is melted to form the liquid.

Figure 3 shows the heat flux versus temperature curve for the melting of a solid that is a mixture of two different phases with differing compositions (say α and β). This solid, when it melts, forms only one liquid phase. This figure clearly shows two different peaks corresponding to the two different phases. At T_1, one of the solid phases (say α) is completely melted, and at this temperature an equilibrium exists between the solid β and the liquid. T_1 corresponds to instant melting of the phase α. (It is quite possible that the melting of the phase α may be similar to Figure 2 if the phase α happens to be a solid solution itself.) Above T_1, the heat-flux signal corresponds to the gradual melting of solid β which is now in equilibrium with the liquid. When all the solid β has melted away, we observe a sharp fluctuation in the heat-flux signal at T_2. This is the final temperature in this phase transition. While it is possible that the heat flux versus temperature curve may be more complicated for a given sample, the two curves discussed here clearly show the idea behind the identification of the solid to liquid transition temperatures.

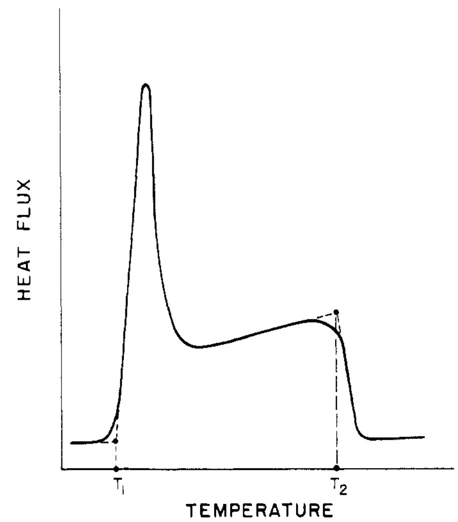

Figure 3. Schematic diagram of the heat flux versus temperature of a system that forms two solid phases.

Table I. Solid-Liquid Equilibrium Data for the Fluorene-Dibenzofuran System: Dibenzofuran Mole Fractions and Initial and Final Temperatures of the Phase Transitions

dibenzofuran mole fracn	init temp/K	final temp/K	type
0.000	387.9	387.9	
0.104	380.8	384.5	solid solution
0.162	376.8	381.8	solid solution
0.272	371.3	378.8	solid solution
0.345	366.9	375.1	solid solution
0.481	360.8	368.3	solid solution
0.602	359.3	363.3	solid solution
0.687	357.5	359.8	solid solution
0.738	357.3	358.3	solid solution
0.812	356.5	357.3	solid solution
0.881	355.6	356.3	solid solution
0.912	355.3	355.9	solid solution
1.000	355.3	355.3	

On the basis of these ideas, by examining the heat-flux signals from many samples with different compositions, we can construct the phase diagrams of the three binary systems studied.

Results and Discussion

Table I shows the solid-liquid equilibrium data obtained for the binary system of fluorene-dibenzofuran. The calorimetric studies also show that this system forms a solid solution at any composition. These data were then plotted in Figure 4. Since we have a simple system, we did some modeling on this binary system. The lines on Figure 4 were obtained by assuming the liquid to be ideal and by modeling the solid using Guggenheim's

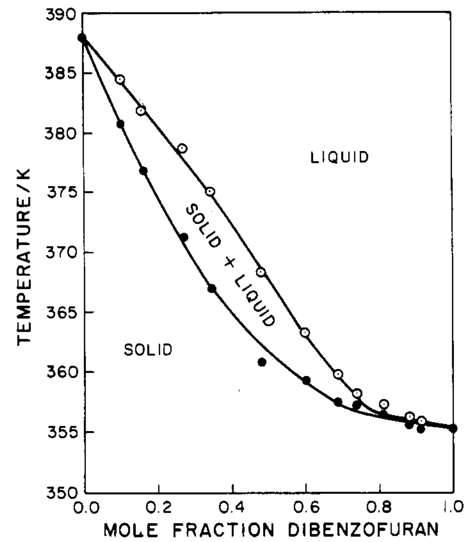

Figure 4. Solid-liquid phase diagram of the fluorene-dibenzofuran system. The lines are predicted by assuming an ideal liquid and a Guggenheim's solid with temperature-dependent interchange energy parameter (w/k) in the form of $w/k = 1896 - 4.73T$.

Table II. Solid-Liquid Equilibrium Data for the Debenzothiophene-Dibenzofuran System: Dibenzofuran Mole Fractions and Initial and Final Temperatures of the Phase Transitions

dibenzofuran mole fracn	init temp/K	final temp/K	type
0.000	371.9	371.9	
0.040	368.9	370.5	solid solution
0.049	368.3	370.0	solid solution
0.077	362.0	367.8	two solid phases
0.114	362.1	366.4	two solid phases
0.135	362.1	365.9	two solid phases
0.177	360.3	362.9	solid solution
0.249	358.1	360.7	solid solution
0.329	356.5	358.7	solid solution
0.400	355.7	357.2	solid solution
0.501	354.6	355.6	solid solution
0.566	354.2	354.8	solid solution
0.648	353.7	354.4	solid solution
0.781	353.6	354.2	solid solution
0.860	353.9	354.4	solid solution
1.000	355.3	355.3	

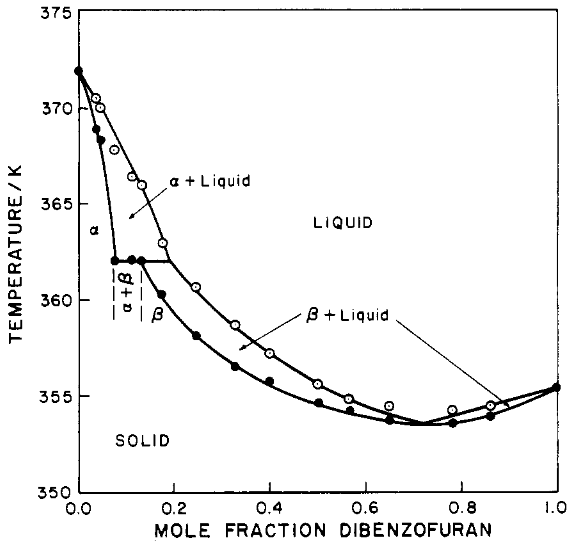

Figure 5. Solid-liquid phase diagram of the dibenzothiophene-dibenzofuran system.

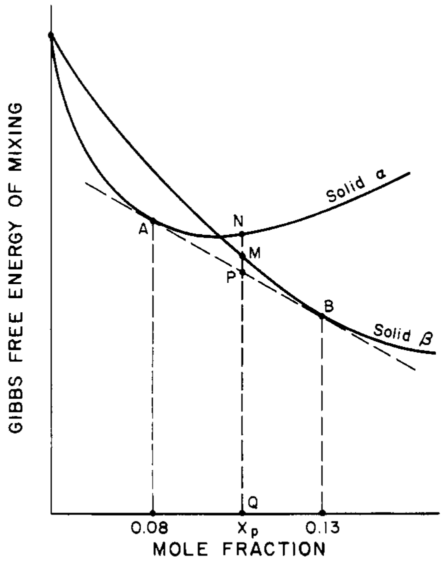

Figure 6. Schematic diagram of the Gibbs free energies of mixing of solid α and solid β versus temperature.

quasi-chemical theory (*4*), with a temperature-dependent interchange energy parameter (w/k). In this modeling, the heats of fusion of the fluorene and dibenzofuran were 19.2 and 18.6 kJ/mol, respectively, and the differences in the liquid and solid heat capacities of fluorene and dibenzofuran were 1.98 and 9.6 J/(mol·K), respectively. Those values were also obtained by the C-80 Setaram calorimeter.

The fact that the fluorene-dibenzofuran system forms solid solutions at any composition is not so surprising, since those two molecules have similar molecular sizes and shapes (Figure 1) and their pure crystals have the same structures, orthorhombic (*10*, *11*).

Table II and Figure 5 show the solid-liquid equilibrium data for the dibenzothiophene-dibenzofuran system. From Figure 5, it can be seen that, for the solid, there are two possible phases. For solid mixtures with dibenzofuran mole fractions less than about 0.08, there is one solid phase (say α), and for solid mixtures with dibenzofuran mole fractions greater than about 0.13, there is another solid phase (say β). In the region, with dibenzofuran mole fractions between 0.08 and 0.13, there is an immiscibility gap in the solid. In this region, the solid consists of solid α and solid β which are mixed. That means that, at those mole fractions, the Gibbs free energy of mixing of solid α and that of solid β are greater than the Gibbs free energy of mixing of a mixture of solid α with dibenzofuran mole fraction 0.08 and solid β with dibenzofuran mole fraction 0.13, that is, having the same bulk dibenzofuran mole fraction.

This situation can be illustrated in a clearer way by Figure 6. This figure shows the expected solid Gibbs free energies of mixing of solid α and solid β as functions of the mole fractions. Suppose that there is a mixture of dibenzothiophene and dibenzofuran with dibenzofuran mole fraction X_p. If the mixture forms solid α, the Gibbs free energy of mixing would be QN, and if the mixture forms solid β, the Gibbs free energy of mixing would be QM. However, if it forms a mixture of solid α with dibenzofuran mole fraction 0.08 and solid β with dibenzofuran mole fraction 0.13, the Gibbs free energy of mixing would be QP, which is smaller than QM and QN, and in fact is the minimum Gibbs free energy of mixing, so that this is what really happens. The proof of this can be found, for example, in Gordon (*12*). The ratio of the amounts of solid α and solid β can be represented by the ratio of the lengths of PB/PA.

As we can see in Figure 5, even though dibenzothiophene and dibenzofuran have similar molecular sizes and shapes, their mixtures have a small immiscibility gap. This was caused by the difference in their pure crystal structures; pure dibenzofuran forms an orthorhombic crystal structure, while pure dibenzo-

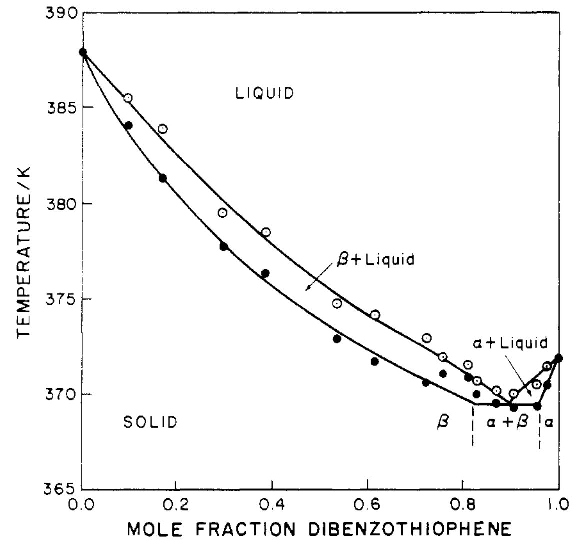

Figure 7. Solid-liquid phase diagram of the fluorene-dibenzothiophene system.

Table III. Solid-Liquid Equilbria Data for the Fluorene-Dibenzothiophene System: Dibenzothiophene Mole Fractions and Initial and Final Temperatures of the Phase Transitions

dibenzothiophene mole fracn	init temp/K	final temp/K	type
0.000	387.9	387.9	
0.097	384.1	385.5	solid solution
0.171	381.3	383.9	solid solution
0.298	377.7	379.5	solid solution
0.387	376.3	378.5	solid solution
0.535	372.9	374.7	solid solution
0.614	371.7	373.4	solid solution
0.722	370.6	372.9	solid solution
0.759	371.1	371.9	solid solution
0.811	370.9	371.6	solid solution
0.830	370.0	370.7	two solid phases
0.870	369.5	370.2	two solid phases
0.907	369.3	370.1	two solid phases
0.955	369.3	370.5	two solid phases
0.978	370.5	371.4	solid solution
1.000	371.9	371.9	

thiophene forms a monoclinic crystal structure (*11*). It can be concluded that solid α has a crystal structure similar to that of pure dibenzothiophene, while solid β has a crystal structure similar to that of pure dibenzofuran.

The data obtained for the last binary system, fluorene-dibenzothiophene, are shown in Table III and Figure 7. Since pure fluorene and dibenzothiophene have different crystal structures, it can be predicted that the fluorene-dibenzothiophene system would have a solid immiscibility gap. This is what we see in Table III and Figure 7. The immiscibility gap lies between mole fractions 0.82 and 0.96 of dibenzothiophene. The same explanation as that in the dibenzothiophene-dibenzofuran system can be applied here. We can also conclude that the solid phase formed at dibenzothiophene mole fractions below 0.82 has a crystal structure similar to that of the pure fluorene, while the solid phase formed at dibenzothiophene mole fractions above 0.96 has a crystal structure similar to that of dibenzothiophene.

Acknowledgment

W.B.S. acknowledges a graduate fellowship from the IXth (Indonesian) World Bank Education Project.

Registry No. Fluorene, 86-73-7; dibenzofuran, 132-64-9; dibenzothiophene, 132-65-0.

Literature Cited

(1) Goldstein, R. F. *The Petroleum Chemicals Industry*; Wiley: New York, 1958.
(2) Sullivan, R. F. *Upgrading Coal Liquids*; ACS Symposium Series 156; American Chemical Society: Washington, DC, 1981.
(3) Whitehurst, D. D. *Coal Liquifaction Fundamentals*; ACS Symposium Series 156; American Chemical Society: Washington, DC, 1981.
(4) Prausnitz, J. M.; Lichtenthaler, R. N.; de Azevedo, E. G. *Molecular Thermodynamics of Fluid Phase Equilibria*, 2nd ed.; Prentice-Hall: Englewood Cliffs, NJ, 1986.
(5) Choi, P. B.; McLaughlin, E. *Ind. Eng. Chem.* **1982**, *22*(1), 46.
(6) Gmehling, J. G.; Anderson, T. F.; Prausnitz, J. M. *Ind. Eng. Chem. Fundam.* **1978**, *17*, 269.
(7) Karunakaran, K. *J. Solution Chem.* **1981**, *10*, 6, 431.
(8) Parrish, Wm. R. *Fluid Phase Equilib.* **1986**, *29*, 177.
(9) Westrum, E. F., Jr. In *Studies in Thermodynamics*; Kehiaian, H. V.; Renon, H., Eds.; Elsevier, Amsterdam, 1985; Vol. 6.
(10) Schudt, E.; Weitz, G. *Structure Data of Organic Crystals*; Springer-Verlag: Berlin-Heidelberg, 1971; Vol. III/5a.
(11) Schudt-Weitz, G.; Stress, I. *Structure Data of Organic Crystals*; Springer-Verlag: Berlin-Heidelberg, 1985; Vol. III/10a.
(12) Gordon, P. *Principles of Phase Diagrams in Materials Systems*; McGraw-Hill: New York, 1968.

Received for review August 29, 1988. Accepted January 17, 1989. S.G. and E.McL. are partially supported by the Office of Basic Energy Sciences (Grant DE-FG05-86ER13632) of the U.S. Department of Energy.